

High-frequency conductivity of two-dimensional electrons under weak-localization conditions

S. A. Vitkalov

P. N. Lebedev Physics Institute, Russian Academy of Sciences, 117924 Moscow, Russia
(Submitted 22 September 1995)

Zh. Éksp. Teor. Fiz. **109**, 1846–1858 (May 1996)

The magnetic-field dependence of the real and imaginary parts of the high-frequency (9.5 GHz) conductivity of a two-dimensional electron gas in a AlGaAs/GaAs heterostructure at temperatures from 1.5 to 7 K is measured. We find that in weak magnetic fields at reduced temperatures under conditions such that the frequency of the electromagnetic field is much lower than the frequency of electron collisions, there is appreciable enhancement of the magnetic-field dependence of the imaginary part of the conductivity, which becomes comparable to variations in the real part of the conductivity in the magnetic field. Both the real and imaginary parts of the conductivity are described well by the weak-localization theory at finite frequency. The diffusion coefficient D^{HF} and the phase coherence time τ_{ϕ}^{HF} are found directly from the high-frequency response and are consistent with D^{LF} and τ_{ϕ}^{LF} determined from low-frequency measurements using the Einstein relation for the diffusion coefficient.

© 1996 American Institute of Physics. [S1063-7761(96)02305-0]

1. INTRODUCTION

The discovery of quantum corrections to the conductivity due to localization and interaction effects^{1–3} greatly advanced the understanding of the phenomena occurring in disordered Fermi systems. Experimental work in this area has been concerned mainly with the influence of quantum corrections to the low-frequency response of disordered conductors. Thus, the temperature and magnetic-field dependences of the interference correction to the dc conductivity have been studied thoroughly and extensively. The situation has been totally different in the area of the high-frequency properties of disordered conductors, where experimental investigations of quantum corrections to the conductivity have only been started.⁴ The results of investigations of the high-frequency properties of a two-electron gas under weak-localization conditions are presented in this paper below.

In the semiclassical theory, the conductivity of metals is described by the Drude equation and does not depend on the frequency ω of the electromagnetic field as long as ω is much lower than the frequency of electron collisions $1/\tau_p$: $\omega\tau_p \ll 1$, where τ_p is the momentum relaxation time. Appreciable frequency dispersion of the response (i.e., a delay between the current and the field) appears when the field frequency ω approaches $1/\tau_p$. In the weak-localization theory, additional interference corrections appear in the conductivity of disordered conductors. The magnitude of these quantum corrections depends on τ_{ϕ} , i.e., the phase coherence time of the electronic wave function for electron scattering in the conductor. Under weak-localization conditions, frequency dispersion of the linear response should appear when $\omega\tau_{\phi} \sim 1$.

The pioneering work⁴ on the detection of frequency dispersion in the quantum correction to the conductivity of one-dimensional Ag filaments at a frequency of 1 GHz employed a contact measurement technique: two elastic electrical contacts were clamped against the sample. Since the resistance

of the clamped contacts and the electrostatics near them are fairly unpredictable, additional calibration of the pickup system is required. Calibration is possible when the variations in the conductivity of the sample are small and well defined. Inexact knowledge of the behavior of the conductivity during calibration will result in errors. Another restrictive factor for the two-contact method is that the measurement of small variations in the conductivity of the sample requires very high stability of the resistance of the clamped contacts under variations in the temperature and magnetic field needed during the experiment, i.e., monitoring of the resistance of the contacts is actually required.

These restrictions do not plague the contactless technique used here, which is similar to the standard microwave technique and can therefore be widely employed. This paper presents the results of an investigation of the frequency dispersion of the conductivity of two-dimensional electrons in AlGaAs/GaAs heterostructures at a frequency of 9.5 GHz under weak-localization conditions, and a comparison with the two-dimensional quantum interference correction in a magnetic field.

Some emphasis should also be placed on the difference between investigations of the frequency dispersion of the quantum correction and investigations of the dynamic suppression of weak localization by an alternating electric field,^{5–7} where the alternating field destroys the time reversal symmetry of the system and thereby causes a decrease in the phase coherence time of the electronic wave function. This effect is quadratic in the amplitude of the alternating field E_{ω} , unlike the response investigated in this work, which is linear in E_{ω} .

2. EXPERIMENT

A two-dimensional electron gas in an AlGaAs/GaAs heterostructure is an ideal system for investigating weak localization. First, because of the simple band structure of GaAs,

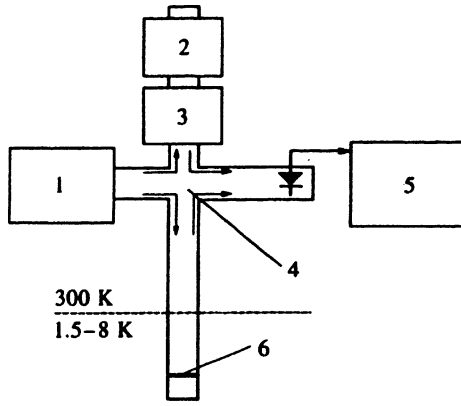


FIG. 1. Schematic representation of the experimental apparatus: 1—high-frequency generator; 2—attenuator; 3—phase shifter; 4—double T bridge; 5—heterodyne receiver; 6—sample.

it has a well defined two-dimensional density of states $N_0 = m^*/\pi\hbar^2$, and there are no complications associated with intervalley scattering. Second, in this system the spin-orbit coupling is negligibly small. Finally, GaAs is a nonsuperconducting material; therefore, there are no corrections to the conductivity due to superconducting fluctuations, and the experiment can be carried out over a broad temperature range.

The AlGaAs/GaAs heterostructures were fabricated by molecular-beam epitaxy and had the following parameters at $T = 4.2$ K, which were determined from low-frequency measurements: sample No. 1—electron concentration $N_e = 8 \times 10^{11} \text{ cm}^{-2}$, mobility $\mu = 48\,900 \text{ cm}^2/\text{V}\cdot\text{s}$; sample No. 2— $N_e = 7.9 \times 10^{11} \text{ cm}^{-2}$, $\mu = 19\,700 \text{ cm}^2/\text{V}\cdot\text{s}$.

The high-frequency conductivity of the heterostructures was determined from the reflection of an electromagnetic field from the samples, which measured $7 \times 15 \text{ mm}^2$ and were placed in a holder across a copper microwave waveguide at an antinode of the electric field. Figure 1 is a block diagram of the apparatus. High-frequency radiation with a frequency of 9.5 GHz was supplied from generator 1 to the E arm of double- T bridge 4. Then half of the microwave radiation was directed into the arm of the T bridge where sample 6 was located. The other half of the microwave radiation entered the compensation arm of the T bridge. The compensation arm contained phase shifter 3 and attenuator 2 and was shorted by a reflecting piston. The electromagnetic radiation reflected from the sample and that reflected from the compensation arm entered the H arm of the T bridge, where the mixer diode of heterodyne receiver 5 was located. The compensation channel can be used to compensate the amplitude of the electromagnetic field reflected from the sample. The pickup system can be tuned to measure the variations in the real (imaginary) part of the reflection coefficient Γ from the sample by introducing additional damping (a phase shift) into the compensation arm.

Relationship between the conductivity $\hat{\sigma}$ and the reflection coefficient Γ of the sample

Let us find the relationship between the reflection coefficient Γ and the conductivity of the sample, which we shall

describe by the tensor $\hat{\sigma} = \sigma_{ij}$, where $i = x, y$ and $j = x, y$. We consider a thin metal film of thickness d placed in the waveguide at a distance L from the plane of the reflecting end of the waveguide. We introduce a rectangular coordinate system: the x axis is parallel to the short wall of the waveguide, the y axis is parallel to the wide wall of the waveguide, and the z axis points in the direction of propagation of the electromagnetic wave. We shall consider the principal wave mode: TE_{10} . The space $0 < z < L$ is filled by an insulator with dielectric constant ϵ . The wave E_x with polarization of the electric field along x propagates along the waveguide (TE_{10} mode). At $0 < z < L$ the field is

$$E_x(0 < z < L) = A_x \sin(k_1 z),$$

where k_1 is the wave vector in the waveguide at $0 < z < L$. This satisfies the boundary condition $E_x(z=0) = 0$ at the totally reflecting end of the waveguide. At $z > L$ the electric field E_x is described by two traveling waves: the wave incident on the sample $E_x^- \exp(ik_2 z)$ and the reflected wave $E_x^+ \exp(ik_2 z)$. The continuity equation of the electric field at $z = L$ gives

$$A_x \sin(k_1 L) = E_x^- e^{-ik_2 L} + E_x^+ e^{ik_2 L} = E_x. \quad (1)$$

A similar expression is obtained for E_y . However, in this case we have two waves damped in both directions from the sample, since the waveguide is cut off for y polarization. At $0 < z < L$ the field E_y equals $A_y \exp[+k_3(z-L)]$, and at $z > L$ it equals $E_y^- e^{-k_4(z-L)}$, where $k_3, k_4 > 0$ are the corresponding wave vectors for y polarization. The continuity equation of E_y near the sample gives

$$E_y(z = L - d/2) = E_y(z = L + d/2) = E_y(L). \quad (2)$$

The equation for the derivatives $\partial E/\partial z$ is easily obtained from the standard wave equation for \mathbf{E} :

$$\nabla^2 \mathbf{E} + \frac{\omega^2}{c^2} \hat{\epsilon} \mathbf{E} = 0,$$

which describes the propagation of an electromagnetic wave in a medium with dielectric tensor $\hat{\epsilon}$. Since the thickness of the sample $d \sim 100 \text{ \AA}$ is much smaller than the characteristic scale field variations in the sample (the depth of the skin layer is $\sim 0.5 \text{ \mu m}$), it can be assumed that the field in the sample does not depend on z . Integrating the wave equation across the thickness of the sample, for the field component E_i we easily obtain

$$\left. \frac{\partial E_i}{\partial z} \right|_{z=L+0} - \left. \frac{\partial E_i}{\partial z} \right|_{z=L-0} = -i \frac{4\pi\omega}{c^2} \sigma_{ij}^{2D} E_j(L). \quad (3)$$

Here we utilized the fact that $\hat{\epsilon} d = i(4\pi\hat{\sigma}/\omega)d = i(4\pi\hat{\sigma}^{2D}/\omega)$.⁸ Substituting the functional dependence $E_i(z)$ into (3) we obtain a system of four linear algebraic equations (1)–(3). From this system we can easily obtain the reflection coefficient

$$\Gamma = E_x^+ e^{ik_2 L} / E_x^- e^{-ik_2 L}$$

of the sample at $z = L$:

$$\Gamma = - \frac{k_1 \cos(k_1 L) + (\beta_{xx} + ik_2) \sin(k_1 L)}{k_1 \cos(k_1 L) + (\beta_{xx} - ik_2) \sin(k_1 L)}, \quad (4)$$

where

$$\beta_{xx} = \alpha_{xx} - \frac{\alpha_{xy}\alpha_{yx}}{k_3 + k_4 + \alpha_{yy}}, \quad \alpha_{ij} = -i \frac{4\pi\sigma_{ij}^{2D}}{c} \frac{\omega}{c}.$$

In the experiment the sample was positioned at $z = \pi/2k_1$, i.e., an antinode of the electric field. In this case

$$\Gamma = \frac{k_2 - i\beta_{xx}}{k_2 + i\beta_{xx}}. \quad (5)$$

In zero magnetic field the conductivity tensor becomes diagonal: $\sigma_{xy} = -\sigma_{yx} = 0$. If $H = 0$, the quantity

$$i\beta_{xx} = \frac{4\pi\sigma_{xx}^{2D}}{c} \frac{\omega}{c}$$

is a positive real number when $\omega\tau_p \ll 1$, since in this case $\sigma_{xx}^{2D} = N_e e^2 \tau_p / m$ is real with a relative accuracy $\omega\tau_p \sim 0.04$. With this degree of accuracy it can be assumed that the reflection coefficient $\Gamma(H=0)$ is real, according to (5).

When a magnetic field is introduced, off-diagonal components σ_{xy} , $\sigma_{yx} \sim H$ appear, as does a magnetic-field dependence of the diagonal conductivity components. The conductivity tensor consists of two parts: the classical conductivity $\hat{\sigma}_{\text{clas}}$ and the conductivity due to the weak localization of the quantum correction $\hat{\sigma}_{\text{wl}}$, which is diagonal. When a magnetic field is introduced, both parts begin to vary.

Let us now consider the classical behavior. The contribution of the quantum correction in the conductivity to the reflection coefficient will be considered below. The conductivity for a one-valley isotropic conductor in a magnetic field is⁹

$$\hat{\sigma}^{2D} = \begin{pmatrix} \sigma_{xx} & \sigma_{xy} \\ \sigma_{yx} & \sigma_{yy} \end{pmatrix} = \frac{1}{(\rho_0^2 + \rho_1^2)} \begin{pmatrix} \rho_0 & -\rho_1 \\ \rho_1 & \rho_0 \end{pmatrix}, \quad (6)$$

where ρ_0 is the resistance per square of the sample when $H=0$, and $\rho_1 = H/N_e e c$. For classically weak fields ($\Omega_c \tau_p \ll 1$, where Ω_c is the cyclotron frequency) the conductivity variations in a magnetic field are small compared with $\sigma^{2D}(H=0)$. In this case the variation of the reflection coefficient (5) in a magnetic field can be represented in the form

$$\begin{aligned} \delta\Gamma_{\text{clas}}(H) &= \Gamma(H) - \Gamma(0) \\ &= \frac{2k_2}{(k_2 + \gamma)^2} \frac{\gamma K^2 + i\gamma^2 K}{K^2 + \gamma^2} \left(\frac{\rho_1}{\rho_0} \right)^2. \end{aligned} \quad (7)$$

Here $\gamma = 4\pi\omega/\rho_0 c^2$ and $K = k_3 + k_4$. It is seen that the variations in the real and imaginary parts of the reflection coefficient are proportional to the square of the magnetic field. As can easily be seen from (4), in the case of arbitrary positioning of the sample and small variations in $\hat{\sigma}$, the functional dependence of the real and imaginary parts of $\delta\Gamma_{\text{clas}}$ on the magnetic field remains unchanged and proportional to H^2 : $\delta\Gamma_{\text{clas}} = \alpha H^2$, where the complex coefficient α depends on L .

Let us evaluate the influence of the quantum correction on the reflection coefficient Γ for the purpose of determining the requirements imposed on the characteristics of the ex-

perimental apparatus. The resistance per square of the heterostructures investigated was $R^{2D} \sim 200-400 \Omega$. The magnitude of the quantum correction to the conductivity is of the order of $\delta\sigma_{\text{wl}} \sim 10^{-5} \Omega^{-1}$ (Ref. 2). It follows from (5) that variations in the reflection coefficient due to the quantum correction are of the order of $\delta\Gamma \sim 10^{-3}$. The measurement of such variations with a relative accuracy of 0.01 requires an accuracy for the measurement of the reflection coefficient of about 10^{-5} . The amplitude fluctuations of the high-frequency generator (a Gunn diode was used) were insignificant for measuring variations in the real part of the reflection coefficient with the required accuracy, since the reflected signal from the sample was compensated by the reflected signal from the compensation channel and the amplitude fluctuations of the field were then also compensated. To measure variations in the imaginary part of the reflection coefficient with an accuracy of 10^{-5} the frequency of the generator was stabilized by a high- Q resonator with 2-4 kHz bandwidth. As the external magnetic field varied during the experiment, the conductivity of the sample also varied. This variation caused an imbalance in the T bridge and was detected by the pickup system.

To vary and monitor the temperature, the sample was placed in a teflon holder along with a resistance thermometer and a heating element, which were in thermal contact with the sample through a heat-transferring sapphire rod. The thermometer and the heating element were placed outside the waveguide. They neither responded to the microwave field, which is important for correct monitoring of the temperature, nor did they make a spurious contribution to the microwave reflection. The waveguide with the sample was placed in a thermally insulated metal tube and immersed in an atmosphere of gaseous ^4He . The entire structure was placed in a cryostat with the solenoid. The accuracy of the temperature stabilization was better than 0.05 K over the entire temperature range investigated. After the high-frequency measurements, indium contacts were prepared on the samples, and low-frequency conductivity investigations were performed at a frequency of 215 Hz by the four-probe method.

3. QUANTUM CORRECTION TO THE CONDUCTIVITY AT FINITE FREQUENCY ω

In the case of temporal dispersion the linear response at time t is determined by the integral of the response function over all preceding times (Ref. 8). In the case of weak localization the correction to the current j_{wl} at time t is

$$\delta j_{\text{wl}}(t) = \int_{-\infty}^t \delta\sigma_{\text{wl}}(t-t_i) E_{\omega}(t_i) dt_i, \quad (8)$$

where¹⁰

$$\delta\sigma_{\text{wl}}(t) = A(t) [e^{-t/\tau_{\varphi}} - e^{-t/\tau_p}]. \quad (9)$$

The quantity $A(t)$ in (9) describes the temporal evolution of the electronic wave function when an electron moves along random interfering trajectories. The function $A(t)$ also takes into account the influence of a magnetic field on the electron interference. The term $e^{-t/\tau_{\varphi}}$ in square brackets describes the damping of phase correlations of the wave func-

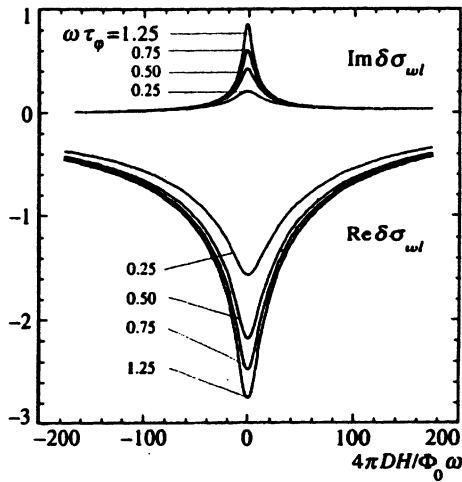


FIG. 2. Theoretical dependence on the magnetic field of the real and imaginary part of the quantum interference correction to the conductivity of a two-dimensional electron gas (in units of $e^2/\pi h$) for various values of $\omega\tau_\varphi$.

tion. The second term in square brackets stems from the requirement that a quantum correction appear at times greater than τ_p . Performing some algebraic transformations in (8) and utilizing the periodicity of $E_\omega(t) = E_\omega e^{-i\omega t}$, we can easily establish that the quantum correction to the conductivity at finite frequency and with $\omega\tau_p \ll 1$ is

$$\delta\sigma_{\text{wl}}(\omega, \tau_\varphi) = \delta\sigma_{\text{wl}}(0, \tau_\varphi^*), \quad \frac{1}{\tau_\varphi^*} = \frac{1}{\tau_\varphi} - i\omega. \quad (10)$$

Thus, the expression for the correction to the conductivity at finite frequency reduces to the expression for the quantum correction to the dc conductivity, but $1/\tau_\varphi$ must be replaced by $1/\tau_\varphi^* = 1/\tau_\varphi - i\omega$. If ωT_p is small, additional corrections to $1/\tau_\varphi^*$ of order $\omega^2\tau_p$ appear. They can be important when $\omega\tau_\varphi \geq 1$, but they are negligible in our work. Using the known expression for the correction to the conductivity of a two-dimensional electron gas in a magnetic field¹¹ and replacing $1/\tau_\varphi$ by $1/\tau_\varphi^* = 1/\tau_\varphi - i\omega$, we obtain

$$\delta\sigma_{\text{wl}}^{2D}(\omega, H) = \frac{e^2}{2\pi^2\hbar} \left[\psi\left(\frac{1}{2} + \frac{\hbar c}{4eDH\tau_\varphi^*}\right) - \psi\left(\frac{1}{2} + \frac{\hbar c}{4eDH\tau_p}\right) \right], \quad (11)$$

where $\psi(z)$ is the digamma function of the complex argument z . Figure 2 presents theoretical plots constructed according to Eq. (11) of the magnetic-field dependence of the real and imaginary parts of the quantum interference correction for different values of $\omega\tau_\varphi$.

4. RESULTS AND DISCUSSION

Figure 3 presents the real part of the reflection coefficient $\text{Re}\delta\Gamma$ of AlGaAs/GaAs heterostructure at an 9.5 GHz and the reciprocal of the resistance per square R^{2D} of a film measured at 217 Hz as functions of the external magnetic field H . Figure 3 shows the difference in the behavior of the

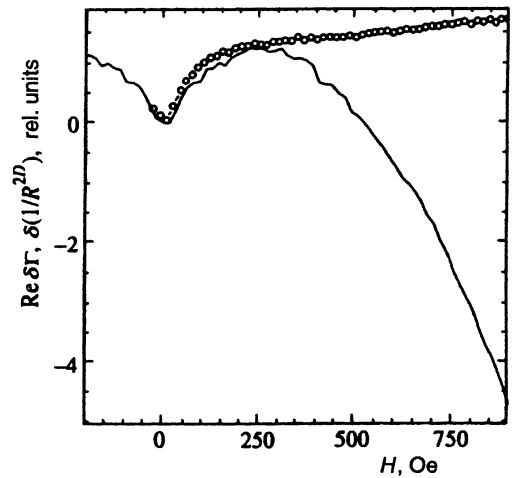


FIG. 3. Magnetic-field dependence of the real part of the reflection coefficient at 9.5 GHz (solid curve) in relative units, and magnetic-field dependence of the reciprocal of the resistance of two-dimensional electrons at 217 Hz (symbols). AlGaAs/GaAs heterostructure at $T=4.2$ K, sample No. 1.

linear response at high and low frequencies in strong magnetic fields. The difference in behavior stems from the fact that at high frequencies the linear response is measured in a given electric field E_ω , i.e., the conductivity (conductance) of the sample σ is measured according to (5). At low frequencies the amplitude of the current through the sample is fixed, and the voltage on the potential contacts is measured, i.e., the resistance R of the sample is measured. Classical magnetoresistance is not observed in a one-valley conductor.⁹ This is because the additional current along the sample due to the Hall voltage exactly compensates the current decrease caused by the deviation of the electron trajectory produced by the magnetic field. Therefore, at low frequencies only the variation of the quantum localization correction is measured, and an approximately constant resistance is observed in strong magnetic fields (Fig. 3), in which the quantum correction to the conductivity is essentially completely suppressed.

In the high-frequency case the variation of both the quantum correction to the conductivity and the classical magnetoconductivity are measured. The change in the reflection coefficient (5) in a magnetic field due to the variation of the quantum correction to the conductivity is

$$\delta\Gamma_{\text{wl}} = A \delta\sigma_{\text{wl}}, \quad (12)$$

where $A = -8\pi k_2\omega/[c^2(k_2 + \gamma)^2]$ is a real number. The total change $\delta\Gamma(H)$ in the reflection coefficient in a magnetic field equals the sum of the contributions (12) and (7):

$$\delta\Gamma(H) = \delta\Gamma_{\text{wl}}(H) + \delta\Gamma_{\text{clas}}(H). \quad (13)$$

In strong magnetic fields the quantum correction is suppressed, and the contribution of the classical dependence $\delta\Gamma_{\text{clas}}(H)$ remains.

To isolate the magnetic-field-dependent behavior of the quantum correction from the measured magnetic-field dependence of the reflection coefficient, the latter was approximated by the classical expression (7) $\Gamma(H > 600 \text{ Oe}) = \alpha H^2$ in magnetic fields from 600 to 1600 Oe, at which the quan-

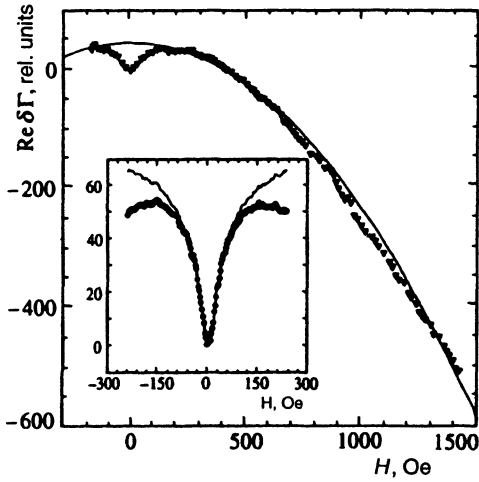


FIG. 4. Magnetic-field dependence of the real part of the reflection coefficient at 9.5 GHz in relative units (symbols), and approximation of this dependence in strong magnetic fields by the classical expression (7) (solid curve). The inset shows the result of subtracting the classical magnetic-field dependence of the reflection coefficient (7) from the experimental curve: upper curve—magnetic-field dependence of the quantum interference correction to the reflection coefficient in relative units. $T=1.49$ K; sample No. 2.

tum correction is essentially completely suppressed, and the coefficient α , which assigns the classical magnetic-field dependence, was determined (Fig. 4). Subtracting the dependence $\delta\Gamma_{\text{clas}}(H)=\alpha H^2$ from the experimental curves, we obtain the dependence $\delta\Gamma_{\text{wl}}(H)$, which, according to (12), is proportional to the changes in the quantum correction to the conductivity in a magnetic field (Fig. 4). The dependence of the quantum correction to the conductivity on the magnetic field obtained as a result of this procedure was used for comparison with theory.

The magnetic-field dependence of the real and imaginary part of the quantum correction to the conductivity of a two-dimensional electron gas in a AlGaAs/GaAs heterostructure at $T=1.5$ K is presented in Fig. 5. The difference in the behavior of the real and imaginary parts of the conductivity is seen from Fig. 5: the imaginary part of the conductivity is suppressed in weak magnetic fields relative to the real part. Such behavior is due to the imaginary part of the quantum correction to the conductivity being formed by trajectories having a length $l_\omega \geq V_F/\omega$, over which an electron moves within a time at least comparable to the period of the electromagnetic field (V_F is the Fermi velocity of an electron). The real part of the quantum correction is produced by all trajectories whose length exceeds the mean free path $V_F\tau_p$. Since $\omega\tau_p \ll 1$, $l_\omega \gg V_F\tau_p$. In the two-dimensional case the area S covered by a random trajectory is proportional to the length of that trajectory. Since the interference is sensitive to the magnetic flux $\Phi=HS$ enclosed by a closed trajectory, the interference is clearly more sensitive to the magnetic field on long trajectories with a length $l_\omega \geq V_F/\omega$ than on short trajectories with a length greater than $V_F\tau_p$ and is therefore destroyed in weak magnetic fields.

The solid lines in Fig. 5 show the results of a comparison with the weak-localization theory (11). Three fitting param-

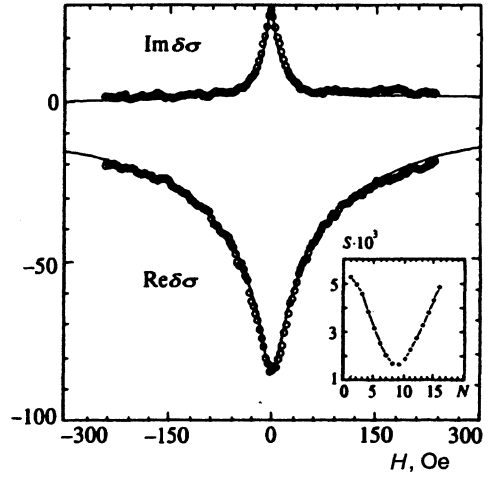


FIG. 5. Magnetic-field dependence of the real and imaginary (upper curve) part of the conductivity of a two-dimensional electron gas in a AlGaAs/GaAs heterostructure at $\omega/2\pi=9.5$ GHz and temperature $T=1.5$ K in relative units. The solid lines depict the results of a comparison with the theoretical equation (11). Parameters obtained: $D^{\text{HF}}(T=1.5\text{K})=499$ cm²/s and $\tau_\phi^{\text{HF}}(T=1.5\text{K})=2.5 \times 10^{-11}$ s. The rms deviation S between the experimental and theoretical curves for various fitting parameters N is shown in the inset. Sample No. 2.

eters were used for each pair (Re and Im) of theoretical curves. One of the fitting parameters, viz., $K_x = \Phi_0\omega/4\pi D$, where Φ_0 is the flux quantum and D is the diffusion coefficient, specified the magnetic-field scale. The other fitting parameter K_y specified the scale of variations in the high-frequency conductivity (the relative variation of the conductivity was measured in the experiment). The phase coherence time τ_ϕ served as the third fitting parameter for finding the best correspondence of the real and imaginary parts of the conductivity to the theory. The real and imaginary parts of the theoretical and experimental curves could not be compared at first. Each experimental curve was approximated by a corresponding theoretical curve, and the fitting parameters K_x^{Re} , K_y^{Re} , K_x^{Im} , and K_y^{Im} for the real and imaginary parts of the conductivity at each value of $\omega\tau_\phi$, which varied discretely with intervals equal to 0.25 over the range 0–1.75, were determined by the least-squares method.

An example of such fitting is shown in the inset in Fig. 5, where the disparity between the theoretical and experimental curves S is plotted along the y axis, and the number N of the trial, which is uniquely related to K_x and K_y , is plotted along the x axis. Then, interpolating the values of K_x^{Re} , K_y^{Re} , K_x^{Im} , and K_y^{Im} with respect to $\omega\tau_\phi$, we determined the value of $\omega\tau_\phi$ at which the disparity between the fitting parameters

$$\Sigma = (K_x^{\text{Re}} - K_x^{\text{Im}})^2 + (K_y^{\text{Re}} - K_y^{\text{Im}})^2$$

is minimal by the least-squares method. The best-fit values for all the curves were 1.8 ± 0.2 for K_x^{Re} and K_x^{Im} and 29.5 ± 3 for K_y^{Re} and K_y^{Im} . At the same time, $\omega\tau_\phi$ varied by a factor of 7.5 upon passage from $T=1.5$ K to $T=6.6$ K.

Figure 6 presents plots of the magnetic-field dependence of the real and imaginary part of the high-frequency conductivity of a two-dimensional electron gas in a AlGaAs/GaAs

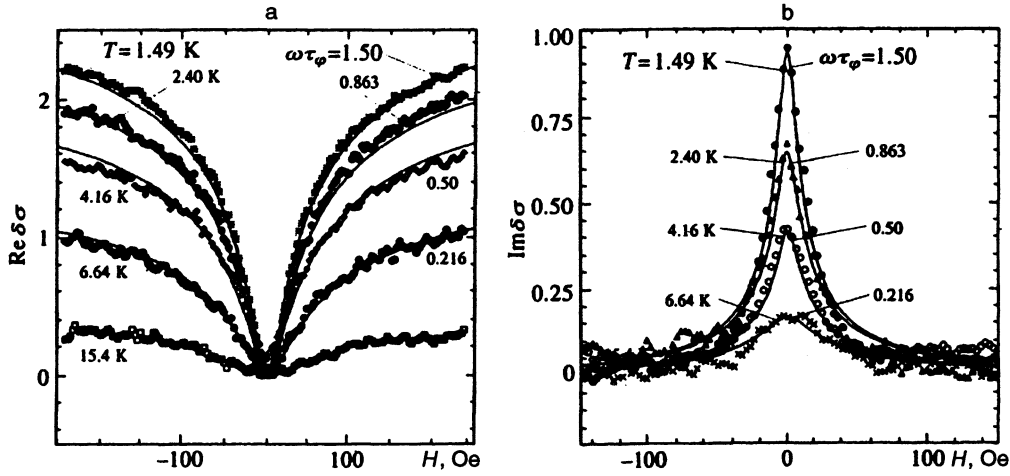


FIG. 6. Dependence of the real (a) and imaginary (b) part of the conductivity of two-dimensional electrons at 9.5 GHz on the magnetic field at various temperatures. Solid curves—theoretical behavior of the quantum interference correction to the conductivity according to (11). All the experimental curves are scaled along the y axis by a factor of 1/29.5, so that the conductivity is measured in units of $e^2/\pi h$. The theoretical curves are scaled along the x axis by a factor K_x from the range 1.8 ± 0.2 for comparison with experiment. Sample No. 2.

heterostructure at various temperatures. The solid lines show the theoretical behavior of the quantum correction to the conductivity according to (11). All the experimental curves in the figures were scaled along the y axis by the mean coefficient $1/K_y^{\text{fit}} = 1/29.5$ for all the curves, which was obtained as a result of comparison with the theory (11). Each pair (Re and Im) of theoretical curves corresponding to a definite value of $\omega\tau_\phi$ was scaled along the x axis by K_x from the range 1.8 ± 0.2 . Thus, all the curves at different temperatures are accurately approximated by the theory when only two scale fitting parameters, viz., K_x^{fit} along the x axis and K_y^{fit} along the y axis, are used and the corresponding value of $\omega\tau_\phi$ is selected. The small spread of the values of K_x and K_y attests to the stability of the procedure used for comparison with theory. At the same time, the small variation of the optimum scale factor $K_x^{\text{fit}} = \Phi_0\omega/4\pi D$ with temperature attests to the weak temperature variation of the diffusion coefficient D , as it should be in a degenerate Fermi gas. The scale factor $K_y^{\text{fit}} = 29.5$ specifies the conversion of the variation of the reflection coefficient $\delta\Gamma_{\text{wl}}$ into the magnitude of the variation of the conductivity σ_{wl} expressed in units of $e^2/\pi h$. Using this factor in (7) and (12), we can determine the magnitude of the variation of the classical conductivity $\hat{\sigma}_{\text{clas}}$ in the magnetic field, which is also expressed in units of $e^2/\pi h$. Using the value of the resistance per square of the sample at $H=0$, $R^{2D} = 403 \Omega$, for the carrier concentration and mobility we obtain $N_e^{\text{HF}} = 6.7 \times 10^{11} \text{ cm}^{-2}$ and $\mu^{\text{HF}} = 23 \text{ 100 cm}^2/\text{V}\cdot\text{s}$. These values correlate with the values obtained from the low-frequency measurements: $N_e = 7.9 \times 10^{11} \text{ cm}^{-2}$ and $\mu = 19 \text{ 700 cm}^2/\text{V}\cdot\text{s}$.

Figure 7 presents the dependence of the reciprocal of the resistance of two-dimensional electrons in a AlGaAs/GaAs heterostructure on the magnetic field at 4.2 K. The solid curve is the theoretical dependence of the quantum correction to the conductivity at low frequency. Using the Einstein relation, we find $D^{\text{LF}} = 550 \text{ cm}^2/\text{s}$ for the diffusion coefficient from the value of the resistance per square of the structure

$R^{2D} = 403 \Omega$. This value correlates well with the diffusion coefficient obtained from the high-frequency data: $D^{\text{HF}} = \Phi_0\omega/4\pi K_x^{\text{fit}} = 554 \pm 60 \text{ cm}^2/\text{s}$. Comparing the experimental and theoretical dependences of the quantum correction and using the value of D^{LF} , for the phase coherence time we find $\tau_\phi^{\text{LF}} = 0.86 \times 10^{-11} \text{ s}$. This value is close to the phase coherence time obtained from the high-frequency measurements at $T = 4.16 \text{ K}$: $\tau_\phi^{\text{HF}} = 0.84 \times 10^{-11} \text{ s}$.

Thus, the technique employed makes it possible to determine the diffusion coefficient of a conductor by a contactless technique, and apparently to reasonable accuracy, without using the Einstein relation. After determining the conductivity, the density of states of a disordered conductor can be determined by a contactless technique using the Einstein relation.

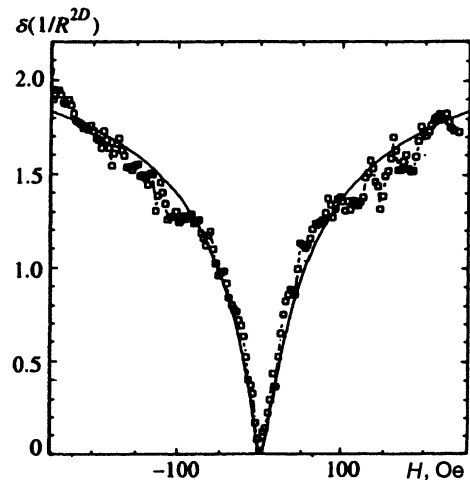


FIG. 7. Dependence of the reciprocal of the resistance per square of a film of two-dimensional electrons (in units of $e^2/\pi h$) on the magnetic field at 215 Hz and $T = 4.2 \text{ K}$. Solid curve—theoretical dependence of the quantum correction to the conductivity on the magnetic field. Sample No. 2.

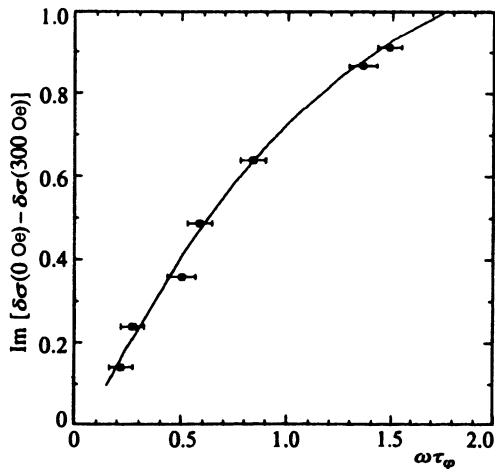


FIG. 8. Imaginary part of the quantum correction to the conductivity (in units of $e^2/\pi h$) at $H=0$ Oe as a function of $\omega\tau_\phi$. Points—imaginary part of the conductivity difference $\sigma(H=0) - \sigma(H=300$ Oe); solid curve—the theoretical dependence (11).

Figure 8 presents the dependence of the imaginary part of the quantum correction to the conductivity on $(\omega\tau_\phi)^{\text{fit}}$ for $H=0$ Oe. The symbols denote the difference between the imaginary parts of the conductivities for $H=0$ Oe and for $H=300$ Oe, at which the imaginary part of the quantum correction is essentially fully suppressed. The solid curve is the theoretical dependence of the imaginary part of the quantum correction on $\omega\tau_\phi$ for $H=0$ Oe.

Figure 9 presents the temperature dependence of the phase coherence time τ_ϕ obtained from high-frequency measurements. The scale of the variations in τ_ϕ with temperature corresponds to the theoretical values for the temperature dependence of τ_ϕ in Ref. 12 and correlates with the temperature dependence of τ_ϕ obtained in Ref. 13 for samples of AlGaAs/GaAs. The value of τ_ϕ obtained from the low-frequency data is denoted in Fig. 9 by a different symbol.

5. CONCLUSIONS

The real and imaginary parts of the high-frequency (9.5 GHz) conductivity of a two-dimensional electron gas in a AlGaAs/GaAs heterostructure in a magnetic field have been measured in the present work by a contactless technique at temperatures from 1.5 to 7 K. It has been found at $\omega\tau_p \ll 1$, but sufficiently low temperatures, that a significant magnetic-field dependence of the imaginary part of the conductivity, which is comparable to the variations in the real part of the conductivity in a magnetic field, appears in weak magnetic fields. Both dependences result from the variation of the quantum interference correction to the conductivity for the finite frequency of two-dimensional electrons in a magnetic field. The experimental results have been compared with the weak-localization theory for $\omega\tau_p \ll 1$ and $\omega\tau_p \sim 1$, and the phase coherence time τ_ϕ^{HF} and the diffusion coefficient D^{HF} , as well as their temperature dependences, have been determined directly. The experimental dependences are described well by the weak-localization theory. The values of D^{HF} and τ_ϕ^{HF} at $T=4.2$ K are consistent with the values of D^{LF} and τ_ϕ^{LF} obtained from low-frequency measurements.

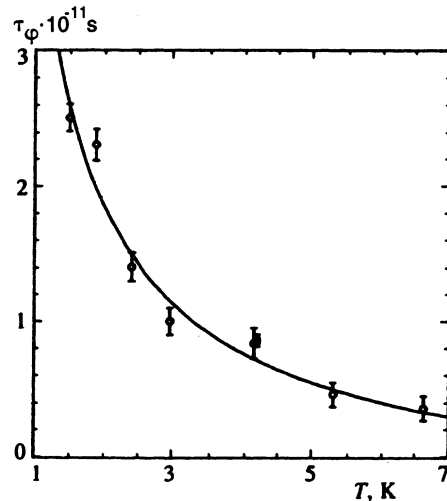


FIG. 9. Temperature dependence of the phase coherence time τ_ϕ^{HF} obtained from conductivity measurements at 9.5 GHz (\circ). The filled box denotes the value of τ_ϕ^{LF} obtained from measurements of the magnetic-field dependence of the conductivity at a low frequency of 215 Hz and $T=4.2$ K. Sample No. 2.

The experimental technique used in the present work can be employed in the contactless determination of the diffusion coefficient and the density of states of disordered conductors, as well as investigations of the dynamic properties of disordered systems.

We thank P. I. Arseev, Yu. M. Gal'perin, and V. I. Fal'ko for useful discussions, V. M. Mishachev and E. G. Sokol for assisting in the experiment, and I. P. Kazakov and V. M. Tsekshosh for the samples provided. This work was carried out with financial support from the Russian Fund for Fundamental Research (Grant No. 94-02-04871-a) and the "Physics of Solid-State Nanostructures" Program (Project No. 1-010).

- ¹ P. W. Anderson, E. Abrahams, and T. V. Ramakrishnan, *Phys. Rev. Lett.* **43**, 718 (1979).
- ² L. P. Gor'kov, A. I. Larkin, D. E. Khmel'nitskiĭ, *Pis'ma Zh. Éksp. Teor. Fiz.* **30**, 248 (1979) [*JETP Lett.* **30**, 228 (1979)].
- ³ B. L. Altshuler, A. G. Aronov, and P. A. Lee, *Phys. Rev. Lett.* **44**, 1278 (1980).
- ⁴ J. B. Pieper, J. C. Price, and J. M. Martinis, *Phys. Rev. B* **45**, 3857 (1992).
- ⁵ S. A. Vitkalov, G. M. Gusev, Z. D. Kvon *et al.*, *Zh. Éksp. Teor. Fiz.* **94**, 376 (1988) [*Sov. Phys. JETP* **67**, 1080 (1988)].
- ⁶ S. Wang and P. E. Lindelof, *Phys. Rev. Lett.* **59**, 1156 (1987).
- ⁷ J. Liu and N. Giordano, *Phys. Rev. B* **43**, 1385, 1991
- ⁸ L. D. Landau and E. M. Lifshitz, *Electrodynamics of Continuous Media*, Pergamon, Oxford (1984).
- ⁹ J. M. Ziman, *Principles of the Theory of Solids*, 2nd. edn., Cambridge Univ. Press, Cambridge, (1972).
- ¹⁰ S. Chakravarty and A. Schmid, *Phys. Rep.* **140**, 193 (1986).
- ¹¹ H. Fukuyama, *Surf. Sci.* **113**, 489 (1982).
- ¹² B. L. Altshuler, A. G. Aronov, and D. E. Khmel'nitskiĭ, *J. Phys. C* **15**, 7367 (1982).
- ¹³ K. K. Choi, D. C. Tsui, and K. Alavi, *Phys. Rev. B* **36**, 7751 (1987).

Translated by P. Shelnitz